JACS
JOURNAL OF THE AMERICAN CHEMICAL SOCIETY

ARTICLE

pubs.acs.org/JACS

Enhanced Hydrolytic Stability of Self-Assembling Alkylated Two-Dimensional Covalent Organic Frameworks

Laura M. Lanni, R. William Tilford, Muktha Bharathy, and John J. Lavigne*

Department of Chemistry and Biochemistry, University of South Carolina, 631 Sumter Street, Columbia, South Carolina 29208, United States

Supporting Information

ABSTRACT: The stability and bulk properties of two-dimensional boronate ester-linked covalent organic frameworks (COFs) were investigated upon exposure to aqueous environments. Enhanced stability was observed for frameworks with alkylation in the pores of the COF compared to nonalkylated, bare-pore frameworks. COF-18Å and COF-5 were analyzed as "bare-pore" COFs, while COF-16Å (methyl), COF-14Å (ethyl), and COF-11Å (propyl) were evaluated as "alkylated-pore" materials. Upon submersion in aqueous media, the porosity of alkylated COFs decreased ~25%, while the nonalkylated COFs were almost completely hydrolyzed, virtually losing all porosity. Similar trends were observed for the degree of crystallinity for these materials, with ~40% decrease for alkylated COFs and 95% decrease for nonalkylated COFs. SEM was used to probe the particle size and morphology for these hydrolyzed materials. Stability tests, using absorbance spectroscopy and ^{1}H NMR, monitored the release of monomers as the COF degraded. While nonalkylated COFs were stable in organic solvent, hydrolysis was rapid in aqueous environments, more so in basic compared to neutral or acidic aqueous media (minutes to hours, respectively). Notably, alkylation in the pores of COFs slows hydrolysis, exhibiting up to a 50-fold enhancement in stability for COF-11Å over COF-18Å.

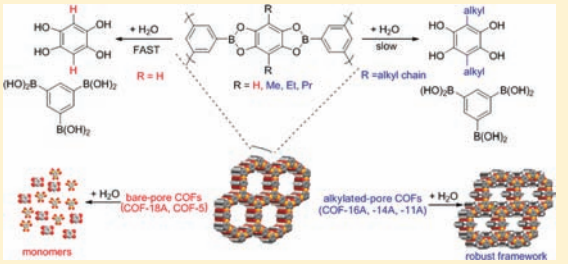

INTRODUCTION

Interest in porous covalent organic frameworks (COFs)[1] has steadily increased since they were first reported in 2005. COFs are insoluble crystalline network solids containing micro- or mesopores exhibiting high surface areas ranging typically from 500 to 1500 m^2 g^{-1}. The highly ordered, uniform, porous architecture found in COFs is analogous to that observed for metal organic frameworks (MOFs).[2] However, because they incorporate only lower molecular weight elements (C, H, O, N, B), COFs are typically lighter than MOFs, making them attractive as platforms for storage, separations, and sequestration of small molecules.[1,3]

A majority of the known frameworks rely on the covalent yet reversible formation of boronate esters as the integral assembly motif. This reversibility of the boronate ester formation is essential for the generation of highly crystalline COFs. However, this crucial and fundamental reversibility cannot be ignored after synthesis. Even though the empty p-orbital on the boron in the integral ester linkage has been shown to be involved in conjugation with the π-electrons on the adjacent oxygen atoms and phenyl rings,[4] it is still susceptible to attack by even modest nucleophiles such as water. As a result, exposure to water, even vapor in the air, could potentially hydrolyze the boronate ester[5] and compromise the integrity of the porous covalent framework, Figure 1. While initial reports proposed that COFs would show enhanced utility as gas storage media because of the reduced density of these materials compared to MOFs, other venues are

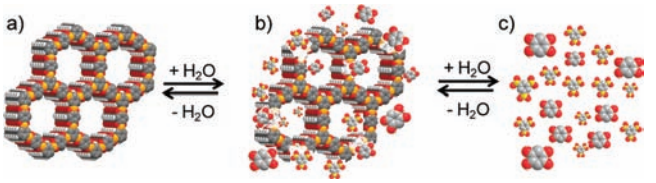

Figure 1. Schematic depiction of (a) insoluble COF, whereupon submersion in water results in (b) partial hydrolysis and release of monomers into solution, until (c) the COF is completely hydrolyzed.

opening up for COF applications. For example, by controlling the rate of hydrolysis of the boronate linkage, these materials could be useful as a platform for controlled release or as the basis for sensor development. Furthermore, controlled hydrolysis could be used as a means to generate other hierarchical structures upon removal of one of the monomers in much the same way that block-co-polymers have been used for this application. Ultimately, the fundamental question of how does one tune/control the rate of decomposition must first be addressed before these materials can find a suitable application. Therefore, understanding and optimizing the hydrolytic stability of boronate ester-linked COFs is essential.

Received: April 25, 2011
Published: August 01, 2011

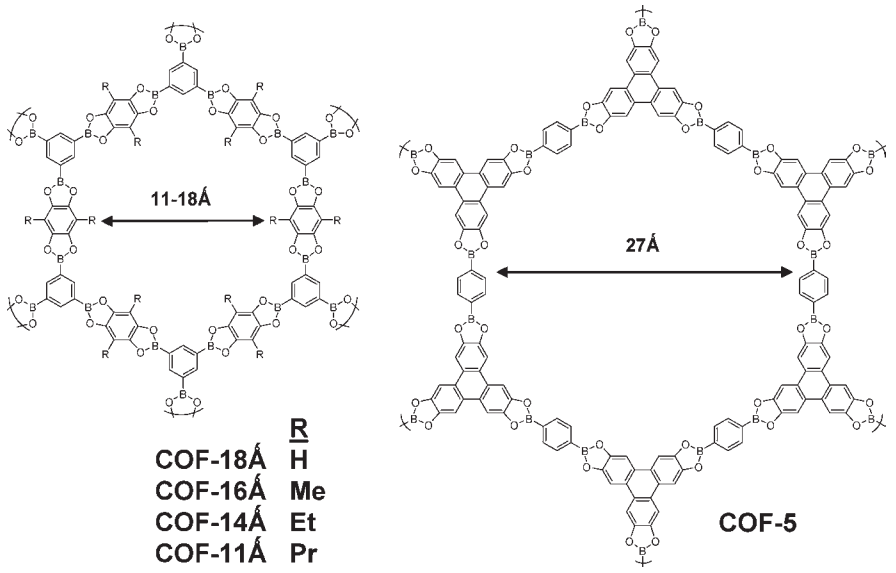

Figure 2. Porous hexagonal structure depicted for COF-18Å, COF-16Å, COF-14Å, COF-11Å, and COF-5. COF-18Å and COF-5 are bare-pore frameworks, whereas COF-16Å (methyl), COF-14Å (ethyl), and COF-11Å (propyl) incorporate hydrophobic alkyl chains in the pores.

While *thermal stability* is generally accepted for both COFs and MOFs, little has been reported on the stability and subsequent properties of MOFs upon exposure to environmental factors, such as water, and to date, there is no data available for COFs. In a recent report, it was shown that the flexible framework of Cu-MOF, $\{[Cu(bpy)(H_2O)_2(BF_4)_2]\}$ (bpy = 4,4′-bipyridine), retained its adsorptive properties upon exposure to water, although its crystalline structure was altered.[6] Another study showed enhanced hydrolytic stability for a multiwalled carbon nanotube-MOF-5 hybrid (MOFMC) over MOF-5 itself.[7] Here it was found that MOF-5 was partially degraded after only 2 h of exposure to 33% relative humidity, whereas the MOFMC showed no degradation even after one week. Related to COFs, we have previously reported on the stability and repair ability of boronate ester-linked linear polymers in solution.[5] Here, polymers showed exceptional stability in organic solvent but were degraded upon exposure to water.

Studies such as these highlight the concerns relating to the stability of these attractive framework structures in practical applications. At the same time, the results described above provide encouragement and suggest that structural modification, for example, incorporation of more "carbonaceous grease," as in the MOF-5/MOFMC example, could help stabilize a framework toward hydrolysis. Previously, it has been shown that alkylation does not alter the planarity of a boronate ester[8] and it has further been demonstrated that short alkyl chains could be included into the pores of planar COFs without altering the general framework geometry.[1c] We thus postulated that incorporation of hydrophobic alkyl chains into the pores of the COF could slow the hydrolysis of the COF by shielding the Lewis acidic boron and thereby providing enhanced hydrolytic stability for COFs.

Herein, the relative rates of hydrolysis are studied for a series of COFs submersed in water. This report specifically details the assessment of the relative hydrolytic stability of nonalkylated and alkylated two-dimensional COFs. The COFs tested in this study included COF-5[1a] and COF-18Å,[1b] which were the first two reported boronate ester-linked COFs. COF-5, like COF-18Å, is a "bare-pore" (nonalkylated) framework. These bare-pore COFs were compared with alkylated COFs structurally analogous to COF-18Å incorporating methyl, ethyl, and propyl substituents into the pores (COF-16Å, COF-14Å, and COF-11Å,[1c] respectively). The adsorption properties, structural ordering, and macroscopic structure of COFs, before and after exposure to water, were assessed. To corroborate this bulk analysis and provide a means to semiquantitatively distinguish differences in stability between COFs, spectroscopic methods (absorbance and NMR) were developed to monitor the release of hydrolysis products into solution, from a solid COF submersed in water. On the basis of this analysis, the relative kinetic parameters for each COF studied and the solvent dependent nature of COF hydrolysis were assessed.

The results suggest that differences in frameworks, such as pore size and monomer hydrophobicity, greatly influence COF stability as well as correlate the impact of hydrolysis on COF structure and adsorption properties. As such, these variables can be altered to modify the framework stability and properties in a predictable manner, thereby providing better control (i.e., more options) when selecting a COF for a specific application.

RESULTS AND DISCUSSION

The previously reported[1b,c] COF-18Å, -16Å, -14Å, and -11Å are made up of hexagonal pores (Figure 2) aligned into channels. The integral boronate ester linkage was formed through the facile condensation reaction between a bis-diol and an aryl triboronic acid. Specifically, 1,3,5-benzene triboronic acid (TBA) was reacted with 1,2,4,5-tetrahydroxybenzene (THB) to provide COF-18Å. Alternatively, the triboronic acid was reacted with 3,6-dialkyl-substituted-1,2,4,5-tetrahydroxybenzenes,[1c] where the alkyl groups include methyl, ethyl, and propyl, resulting in COF-16Å, COF-14Å, and COF-11Å, respectively. The other boronate ester-linked COF depicted in Figure 2 is COF-5. It was the first reported COF and is derived from reaction between 1,4-benzene diboronic acid (BDBA) and 2,3,6,7,10,11-hexahydroxytriphenylene (HHTP).[1a] COF-5 is the most thoroughly studied and reported on material of its kind, having been studied in simulations,[9] as

monolayers on surfaces,[10] and in novel microwave syntheses.[11] It was therefore included as an alternate nonalkylated, two-dimensional, hexagonal COF to evaluate alongside COF-18Å. For comparison, COF-5 was prepared based on the initially published procedure as well as using a procedure to mirror the preparation of COF-18Å.[1b] The products obtained from both of these approaches were indistinguishable from each other and analogous to the originally reported material.[12] As such, the data reported below for COF-5 is from material derived from the synthetic method used for the formation of the other COFs being analyzed.

Bulk Properties of COFs upon Exposure to Water. To investigate the degree of crystallinity and extent of porosity retained after exposure to water, gas adsorption and PXRD analyses were carried out for the unfunctionalized and alkyl functionalized COFs described above. To probe the effect alkylation plays in altering stability toward hydrolysis, COF-14Å was chosen as a "typical alkylated COF" for comparison with COF-18Å. The influence of pore diameter was assessed comparing COF-18Å and COF-5 (18 Å and 27 Å pore diameter, respectively), as "bare-pore," nonalkylated frameworks.

Each COF was encapsulated in filter paper and submerged in water for 20 min without stirring. After this time, the filter papers were removed and air-dried for 30 min and then oven-dried at 110 °C for 1 h. The remaining solids were washed with THF to remove any remaining hydrolysis products, and then dried for 24 h under reduced pressure (~0.5 mmHg). It is noteworthy that these drying conditions have been previously reported as a means of repairing hydrolytically damaged linear poly(boronate)s,[5] thus, framework repair was possible if the hydrolysis was incomplete and the necessary reactants were not washed away.

The percent mass recovered was calculated based on the remaining material on the filter paper at this stage, and is indicative of what portion of the framework was not hydrolyzed. For COF-18Å, 41% of the starting mass was recovered, while for COF-14Å, 84% was recovered, more than twice the amount isolated for the nonalkylated parent framework. During the 20 min aqueous soak, however, COF-5 appeared to be completely hydrolyzed, as no material was collected from the filter paper. Therefore, all post-hydrolysis testing for COF-5 was completed on the dried solids from the THF wash which passed through the filter paper.

Interestingly, during the hydrolysis tests, the color of the water turned pink immediately for COF-18Å, indicating the rapid release and oxidation of THB. However, the water above COF-14Å remained clear and colorless for the entire soak time. It is worth mentioning here that, previously, the extinction coefficients and oxidation parameters were studied for these bis-diol monomers. All of these initial indicators are consistent with the supposition that COF-18Å hydrolyzed more rapidly than COF-14Å during the soak.

Subsequently, the porosity and surface area of the hydrolyzed COFs were assessed based on the nitrogen adsorption properties of the isolated material, while the crystallinity was assessed using powder X-ray diffraction (PXRD). Figure 3a shows the nitrogen adsorption isotherms and Brunauer–Emmett–Teller (BET) surface areas for COF-5 (red), COF-18Å (black), and COF-14Å (blue), before (filled symbols) and after hydrolysis (open symbols). Initially, the nitrogen uptake for the COFs studied, from highest to lowest, was COF-5, COF-18Å, and then COF-14Å. However, after hydrolysis, the relative order of the isotherms was reversed.

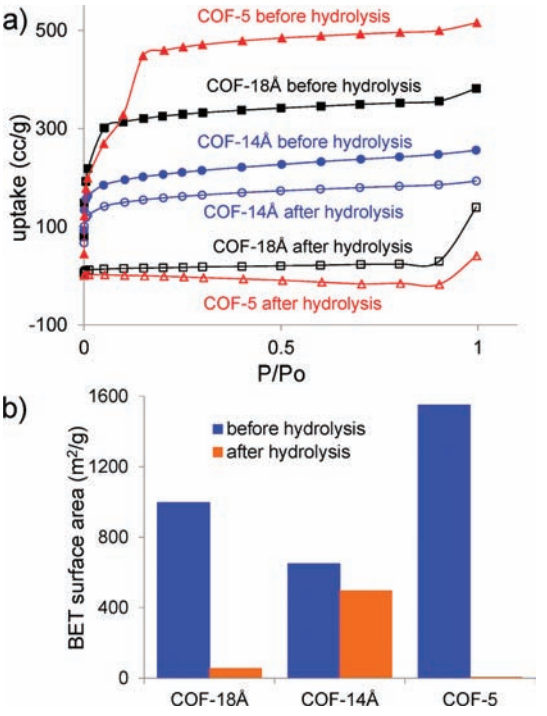

Figure 3. a) Nitrogen adsorption isotherms at 77 K for COF-18Å (black squares), COF-14Å (blue circles) and COF-5 (red triangles), before hydrolysis (filled symbols) and after 20 min hydrolysis (open symbols). b) BET surface area for COF-18Å and COF-5 with non-alkylated pores as well as COF-14Å with ethylated pores, before (blue) and after 20 min hydrolysis (orange).

Following hydrolysis, the integrity of each COF was assessed based on the change in surface area. The bar graph in Figure 3b shows the BET[13] surface area for each COF studied.[14] Before hydrolysis, COF-18Å had a surface area similar to that of previously reported materials,[1b,c] of 996 $m^2\ g^{-1}$ that decreased substantially to 55 $m^2\ g^{-1}$ after hydrolysis, a 95% reduction. Clearly, the microporous framework of this nonalkylated COF was extensively destroyed upon exposure to water. The same was true for the other nonalkylated framework, COF-5. Here the initial surface area of 1550 $m^2\ g^{-1}$ was reduced to zero after hydrolysis, suggesting complete decomposition of the COF. Alkylated COF-14Å, on the other hand, maintained 76% of the initial measured surface area, even after prolonged exposure to water, suggesting a remarkable resistance to hydrolysis. The post-hydrolysis Type I isotherm indicated retention of a robust microporous COF-14Å framework. The surface area for COF-14Å post-hydrolysis was 496 $m^2\ g^{-1}$, which is nearly an order of magnitude higher than the surface area measured for the non-alkylated parent COF-18Å after exposure to water.

The crystallinity of each COF was evaluated before and after hydrolysis, using PXRD (Figure 4). For consistent comparisons, each scan used 30 mg of COF in the same sample holder. Samples were evaluated in the dry state and scanned from 0 to 70° 2θ with a 0.05° step size. The resulting attenuation in the initially high peak intensities after hydrolysis for both nonalkylated frameworks, COF-18Å and COF-5,[15] indicated a complete loss of crystallinity. However, for COF-14Å, this decrease was less perceptible. While the initial PXRD peak intensities for COF-14Å are not as sharp as those for COF-18Å or COF-5, due to the free rotation of the ethyl chains in the pores, after

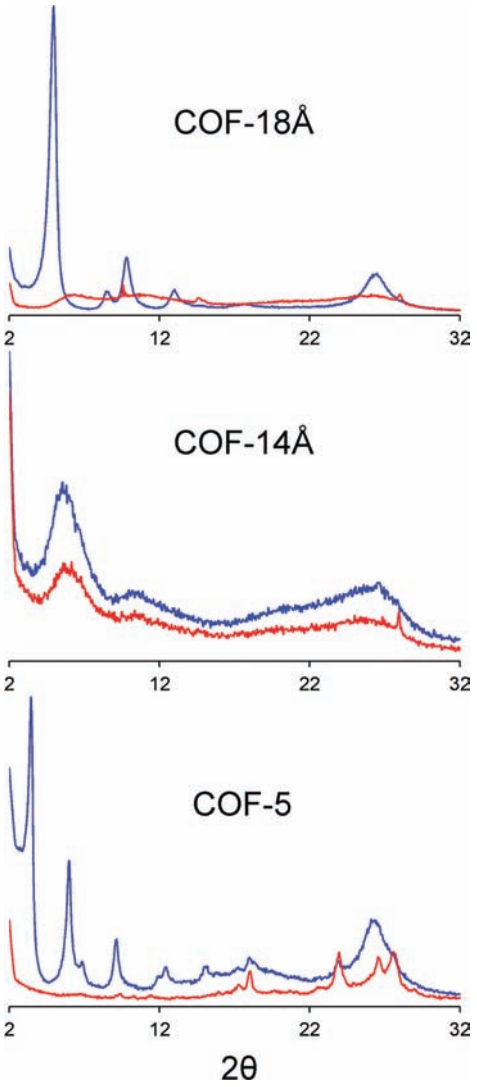

Figure 4. PXRD before (blue) and after (red) hydrolysis for COF-18Å, COF-14Å, and COF-5 indicate complete loss of crystallinity post-hydrolysis for the nonalkylated frameworks, COF-5 and COF-18Å, compared to retention of crystallinity for alkylated COF-14Å.

hydrolysis the peak positions are still identifiable for COF-14Å, implying retention of the crystal packing for this framework.

Scanning electron microscopy (SEM) was used to compare the particle sizes and morphologies of COF-18Å and COF-14Å before and after hydrolysis. Numerous images were analyzed indicating that the initial particle size for each COF averaged from 25 to 30 μm. Representative images are shown in Figure 5a,c. After hydrolysis however, the average particle size for COF-18Å dropped to 10 μm with a much greater size distribution (i.e., particle size dispersity), while the average particle size for COF-14Å was relatively unchanged ($\sim$25 μm).

Likewise, COF-18Å had a considerably different morphology, whereas COF-14Å appeared virtually unchanged. The dried hydrolyzed COF-14Å retained the same particle shape and grainy powder form after the soak as it had before (Figure 5d). However, COF-18Å was darker and appeared finer after hydrolysis (Figure 5b). This was consistent with the noted porosity and crystallinity differences observed between the bare-pore (COF-18Å) and alkylated (COF-14Å) frameworks.

The data summarized in Table 1 suggests that, compared to bare-pore COFs (COF-18Å and COF-5), alkylated COF-14Å exhibits improved hydrolytic stability. This enhanced resistance toward hydrolytic degradation is indicated by the higher percentage of mass recovered, surface area maintained, and crystallinity retained for the alkylated COF-14Å after exposure to water.

Evaluation of Relative Hydrolysis Rates of COFs. On the basis of the impressive differences observed in the bulk properties of COFs after exposure to water and thus the perceived large disparities in stability as a function of alkylation, subsequent work involved additional studies to assess the differences in the rates of COF hydrolysis as a function of pore-alkylation. Specifically, the hydrolytic stability of the COFs was assessed by submerging each insoluble framework in aqueous solution, and upon hydrolysis of the boronate ester linkages, monitoring the release of the hydrolysis products into solution. In parallel analyses, absorbance spectroscopy was used to detect the diol-containing components, while ^{1}H NMR was used to follow the boronic acid building blocks released from the COF into the supernatant solution. These analytical methods were chosen because they each provide unique spectral signals, diagnostic of the targeted hydrolysis products, thereby allowing for straightforward data analysis. Subsequently, differences in the rate of the appearance of the spectral signal for the released COF component correspond to differences in the hydrolytic stability of each framework. Given the lack of precedence for this type of analysis, these dual techniques also serve to corroborate the validity of each approach.

Relative COF Stability by ^{1}H NMR. ^{1}H NMR was used to monitor, over time, the release of the common boronic acid monomer (TBA) in D_2O from ground COF-18Å and COF-14Å samples. Each solid COF was placed in an NMR tube and D_2O was added, using benzene as an internal standard. The appearance and subsequent intensity (integration) changes of the peak at 8.07 ppm, corresponding to the common TBA monomer of COF-18Å and COF-14Å, were monitored with respect to time. This ^{1}H NMR analysis monitored the same monomer (TBA) released from each COF, and thus provided a straightforward assessment of the relative hydrolysis rates between the bare-pore and alkylated frameworks. The aromatic region of the NMR spectra for COF-18Å and COF-14Å is shown in Figure 6a.

As indicated, from bottom to top, times correspond to the initial, 1 h, 1 day, and 1 week measurements. For COF-18Å, the TBA peak was evident immediately. However, for COF-14Å, release of TBA was not noted until 1 h and even then was a small peak. Indeed, at 1 day, the TBA peak for COF-14Å was still not as big as it was for COF-18Å after 1 h. Figure 6b graphically depicts the growth of the TBA peak (derived from integration values referenced to benzene) as a function of time over the first hour for each COF and shows the rapid degradation of COF-18Å compared to the slower hydrolysis of COF-14Å.

Data acquired over 1 week are shown in Figure 6c. As a warning, note that while the rate of hydrolysis of COF-18Å is much faster than that observed for COF-14Å, the intensity of the resonance for each COF reached the same maximum. Given the low solubility of the TBA monomer under these experimental conditions (0.7 mL D_2O added to 1 mg of solid COF in an NMR tube), it is likely that the solutions are simply becoming saturated with TBA and that both hydrolysis studies did not reach the same end point. Still, this study was designed to evaluate the initial kinetics of hydrolysis, and using this small sample size afforded experimental parameters where TBA was fully soluble and assessment of the difference in the relative rate of release of this

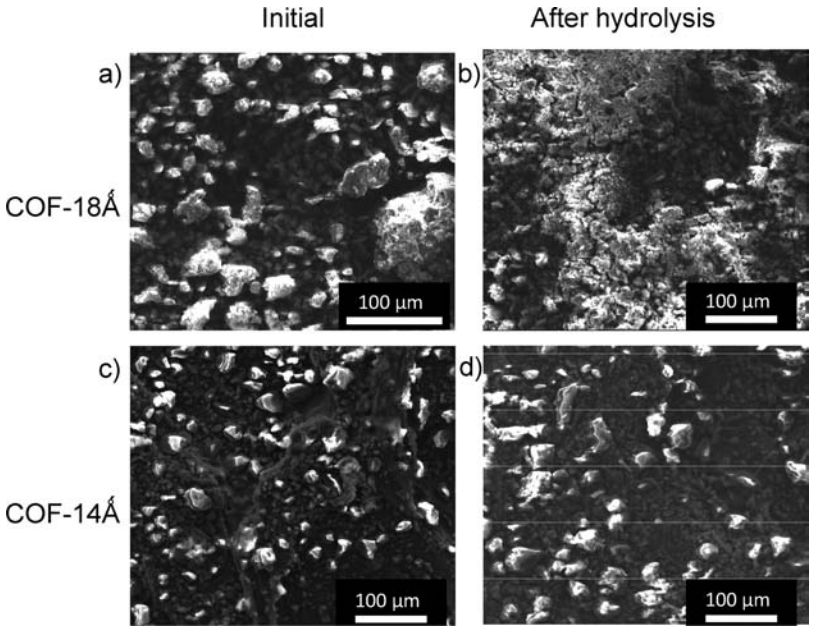

Figure 5. SEM images of COF-18Å (a) before and (b) after hydrolysis, and COF-14Å (c) before and (d) after hydrolysis. The scale indicated on all images is 100 μm. Initial images indicate that the particle diameter for both COFs average 25−30 μm (a and c). However, COF-18Å has a smaller particle size and appeared as a finer grain post-hydrolysis (b compared to a), whereas COF-14Å retains the original size and particle shape post-hydrolysis (d compared to c).

Table 1. Summary of Post-Hydrolysis (20 min Water Soak) Bulk Properties for Alkylated COF-14Å versus Bare-Pore Frameworks COF-18Å and COF-5.

framework	pore size (Å)	pore branching	% mass recovered	% SA_{BET} retained	% particle size retention[a]	% PXRD peak intensity retained[b]
COF-14Å	14	ethyl	84	76	95	57
COF-18Å	18	none	41	5.5	35	4
COF-5	27	none	0	0	—[c]	6

[a] Percent particle sizes were obtained from SEM imaging. [b] Percent peak intensity was calculated from the (100) peak for each COF which gives an indication of the diameter of the pores in the framework. The (100) peaks used for COF-14Å, COF-18Å, and COF-5 were 2θ = 6, 4.95, and 3.5°, respectively. [c] No COF was recovered following hydrolysis.

common monomer was feasible. Thus, the NMR hydrolysis evaluation provides a rapid, small scale method to compare release of monomer in water for the two frameworks which both contain a common monomer, and corroborates the bulk analyses (nitrogen adsorption and PXRD) that alkylation proved to be an effective guard against hydrolysis of the boronate ester-linked framework.

Relative COF Stability by Absorbance Spectroscopy. To corroborate the ^{1}H NMR findings as well as to obtain more rapid data acquisition in order to assess relative initial kinetics, an alternate technique was pursued. Because the monomers used to make two-dimensional COFs absorb ultraviolet light, absorbance spectroscopy was investigated as a rapid detection technique to monitor the release of monomers from COF samples upon hydrolysis. The general experimental approach involved immobilizing clean, dry, ground COF in the bottom of a quartz cuvette by encasing the solid in a precisely folded filter paper. Without some form of containment, the solid COF dispersed in the water forming a cloudy suspension that prohibited transmission-based analysis. Other immobilization methods such as using tea bags were tried but the tea bags were quite delicate and tended to open during testing resulting in "leaks" that caused sudden jumps in the absorbance intensity. However, upon careful addition of solvent to the COF immobilized in the folded filter paper and with periodic monitoring of the solution absorbance above the COF, information was gained about the relative rate of release of the hydrolysis products from the COF into solution.

By following the increase in the intensity of the absorbance at 300 nm, the relative rates of degradation of these COFs were determined. Note that the boronic acid monomers do not absorb in this region while each diol building block has a high extinction coefficient at 300 nm, though this is not necessarily the wavelength of maximum absorbance.[12] Subsequent analysis took into account variation in the extinction coefficient for each different monomer. Furthermore, while the alkyl substituted bis-diols displayed modestly different solubilities in water compared with THB, at the concentrations being evaluated using this approach, there were no appreciable differences observed in solubility, monomer diffusion rate into solution, or monomer retention within the filter paper. Monitoring the active release of monomer and basing the analysis on initial kinetics allowed for determination of THB or dialkyl-THB monomer concentrations before these building blocks auto-oxidized.[16] Note that the observed relative rates correspond to lower limits with respect to COF

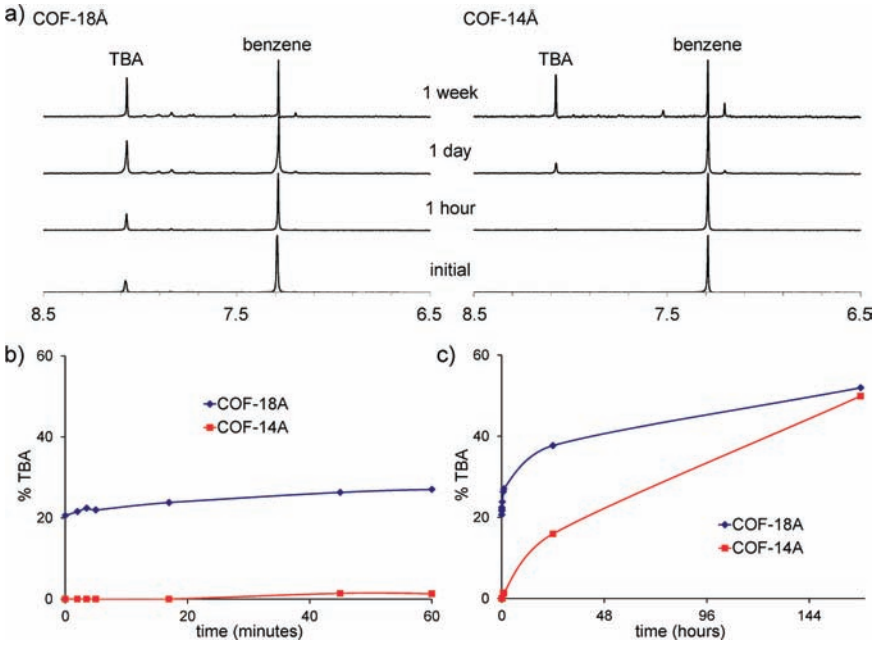

Figure 6. (a) ^{1}H NMR spectra of the aromatic region for COF-18Å and COF-14Å in D_2O at time = 0, 1 h, 1 day, and 1 week. The common monomer, 1,3,5-benzene triboronic acid (TBA), appears at 8.07 ppm. Plot of the % TBA released as a function of time for COF-18Å (blue diamonds) and COF-14Å (red squares) based on ^{1}H NMR analysis in D_2O using benzene as an internal reference for (b) time = 0−1 h, and (c) over 1 week.

stability due to the potential interferences based on the variables cited above (i.e., solubility, diffusion, retention or oxidation). Without any form of agitation, it is important to note that this analysis is diffusion limited, and while the filter paper is likely not homogeneous from sample to sample (or even within the same sample), having a 1 cm^2 surface area is quite large compared to the small amounts of material used, and as such, the statistical variation between samples based on this setup is quite small. For example, in six runs using this approach to assess the stability of COF-18Å, the percent variance was only 2.5% between runs. This method has produced consistent results not only for samples derived from the same synthetic batch of a COF, but also for samples from multiple different batches of the same type of COF.

Impact of Alkylation on COF Stability by Absorbance Spectroscopy. The influence of alkylation in the COF pores was evaluated using the absorbance method described above to compare COF-16Å (methyl), COF-14Å (ethyl), and COF-11Å (propyl) with respect to COF-18Å (bare-pore). All samples were ground to approximately the same size particles to minimize macroscopic variation imparted during synthesis. Figure 7 illustrates that as the length of the alkyl chain was increased, the rate of hydrolysis decreased. Again, it is important to recognize that the rates observed for the hydrolysis of these different COFs are relative to COF-18Å and do not represent absolute rates. Specifically, Figure 7a−c shows the appearance of an absorbance peak centered around 290 nm with respect to time, upon hydrolytic decomposition of COF-18Å, COF-16Å, and COF-14Å in water. The intensity of this absorbance correlates to the amount of bis-diol monomer released into solution as the COFs hydrolyze. Note that COF-11Å is not shown here because it exhibited a smaller increase in this absorbance than COF-14Å.[12] Figure 7d graphically depicts the initial rate of hydrolysis, as derived from the increase in absorbance at 300 nm over time for each COF. This plot highlights the difference in the relative stability between the nonalkylated and the alkylated COFs. Furthermore, the data indicates that longer alkyl chains in the pores inhibit monomer release under hydrolytic conditions, thereby imparting enhanced stability of the COF. This correlates with the bulk adsorption data presented above and can serve as a predictor of COF stability.

On the basis of these analyses, it is possible to monitor the change in bis-diol concentration as a function of time to estimate kinetic parameters (Figure 7d). Here, the slope of the line corresponds to the relative rate of hydrolysis for each framework. As such, COF-18Å hydrolyzed the fastest (steepest slope) followed by COFs-16Å, -14Å, and -11Å, respectively. The slower hydrolysis correlates with increasing alkyl chain length. For example, consider the difference in hydrolysis rate for COF-18 with bare pores compared to COF-14Å with ethyl groups in the pores. Analysis using a pseudo-first-order kinetic model, based on the experimental condition of a large excess of water, the hydrolysis half-life of COF-18Å was calculated to be ∼1 h.[12] Comparatively, COF-14Å had a longer half-life of ∼17 h.[12] Alternatively, if the hydrolysis is modeled as zero-order (reasonable for initial kinetics in this case where the concentration of the COF, an insoluble solid, is exceedingly small), the relative increase in stability is the same; the half-life for hydrolysis of COF-14Å in water is still found to be approximately 20 times longer than that of COF-18Å. These results further confirm that alkyl chains in the COF pores effectively protect the Lewis-acidic boron from hydrolysis and provide an efficient technique for evaluation of differences in stability for this family of COFs.

Impact of Solvent on Nonalkylated COF Stability by Absorbance Spectroscopy. Further analysis of COF-18Å demonstrated variations in stability depending on the pH of the supernatant aqueous solutions as well as verifying the stability of this framework in dry organic solvent. When the absorbance-based method described above was used, the hydrolytic stability of nonalkylated framework COF-18Å was evaluated in base, acid,

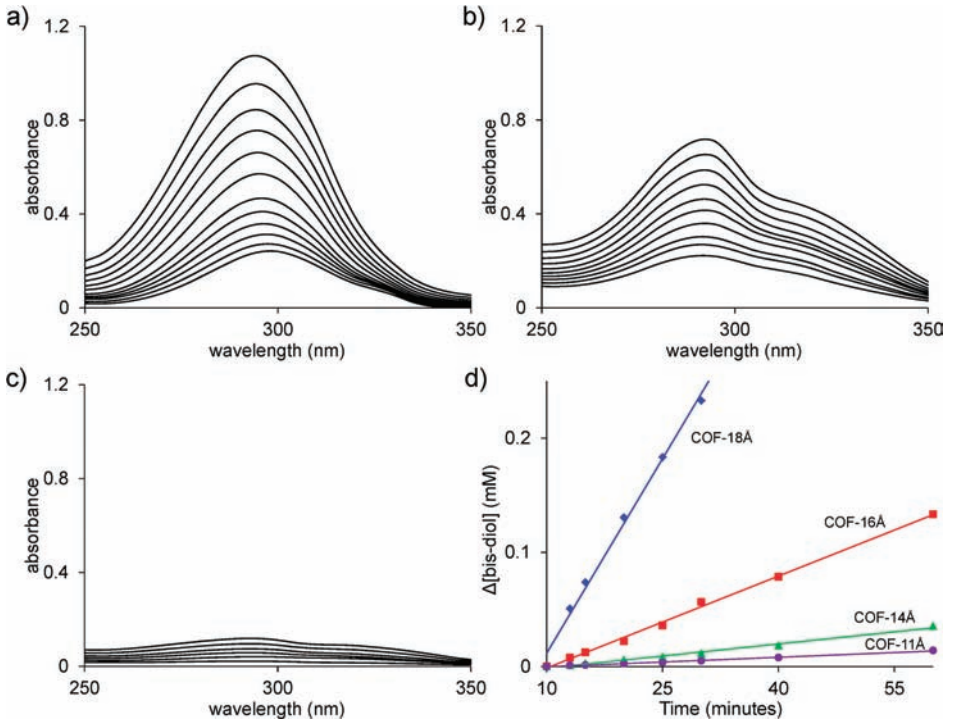

Figure 7. Absorbance spectra showing an increase in the intensity of the peak indicative of the release of bis-diol (300 nm) from the COFs during one hour hydrolysis in water for a) COF-18Å, b) COF-16Å, and c) COF-14Å. COF-11Å showed no appreciable change in absorbance during the one hour test. d) Comparison of the rate of increase in bis-diol concentration correlating to hydrolysis of COF-18Å (blue diamonds), COF-16Å (red squares), COF-14Å (green triangles), and COF-11Å (purple circles) in water.

buffered aqueous solution, water, and 1,4-dioxane. Figure 8 shows the increase in the concentration of THB in the liquid layer above the immobilized COF, as a function of time based on the intensity of the absorbance at 300 nm. In dry 1,4-dioxane, COF-18Å does not hydrolyze, as evidenced by the lack of release of the THB monomer. However, in all aqueous solutions, COF-18Å did hydrolyze, though at varying rates dependent on the solvent system. Under aqueous basic conditions (0.1 M NaOH, pH = 13.3), COF-18Å began to hydrolyze as soon as the solvent was added to the cuvette and the first measurement was obtained. While COF-18Å exhibited similar rates of hydrolysis in aqueous HEPES buffered solution (50 mM HEPES, pH = 7.5), NanoPure water (pH = 7), and aqueous acid (0.1 M HCl, pH = 1), hydrolysis was more gradual compared with the basic conditions.

Also notable was the observed coloration of the supernatant solution after incubation with COF-18Å for 60 min which results from the auto-oxidation of THB over time (Figure 8b). As expected, no color was observed in the dioxane solution and the color appeared immediately under basic conditions. In neutral unbuffered water and HEPES buffered solution, the color appeared more gradually, over the course of minutes. Interestingly, under acidic conditions, the solution was slow to develop any color, and only a light yellow shade was observed after 60 min. While the hydrolysis studies monitoring release of THB at 300 nm suggest that COF-18Å exhibits similar stability trends in neutral unbuffered, neutral buffered, and acidic media, the endpoint color reveals that there is a difference in the stability of the hydrolysis fragments under varying conditions. These results are consistent with the expected protonation state of THB and subsequent auto-oxidation potential at neutral pH compared to low pH[17] and serve to highlight how external conditions need to be carefully evaluated when identifying potential applications for these materials.

The stability of COF-5 was also evaluated in the same five solvents. On the basis of reported structural analyses, both COFs form a two-dimensional array of hexagonal pores large enough to allow water penetration. However, COF-18Å is microporous with 18 Å pores, while COF-5 is mesoporous, containing larger 27 Å pores. Given this pore size disparity and significant differences in the solubility of the hydrolysis products obtained from the two COFs, direct comparison between COF-18Å and COF-5 was difficult. Still, COF-5 generally follows similar trends to those observed for COF-18Å.[12] In particular, COF-5 is least stable under basic conditions and displays similar stability between neutral unbuffered and acidic aqueous solutions.

CONCLUSIONS

In summary, we report on multiple analytical methods showing that alkylation in the pores of the boronate ester-linked COF-18Å family slows hydrolysis likely resulting from a more stable boronate ester linkage in the framework. Bulk hydrolysis of COF-5, COF-18Å, and COF-14Å followed by SEM, PXRD, and gas adsorption analyses revealed the protecting influence of alkylation in the pores in terms of retention of surface area, porosity, crystallinity, particle size, and percent recovery of COF. A rapid and reproducible hydrolytic stability test for COFs was developed requiring small amounts of material for analysis, in which monomer release is monitored over time using absorbance spectroscopy to evaluate the relative rates of COF decomposition, and was corroborated by ^{1}H NMR. These combined studies suggest that upon exposure to water, bare-pore COFs hydrolyze

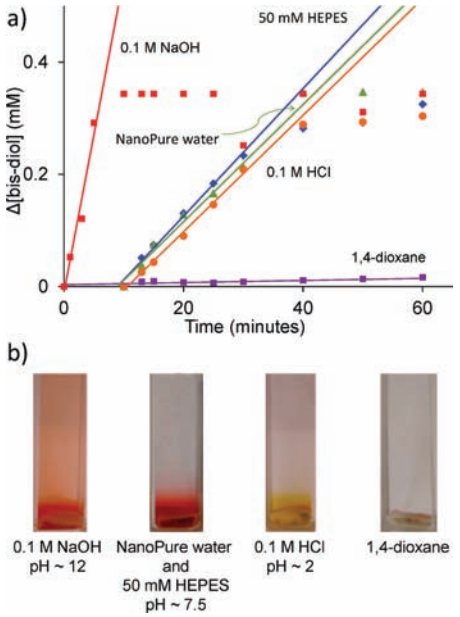

Figure 8. (a) COF-18Å hydrolysis in 0.1 M NaOH (red squares), 50 mM HEPES buffer (blue diamonds), NanoPure water (green triangles), 0.1 M HCl (orange circles), and 1,4-dioxane (purple squares) determined by monitoring the release of THB at 300 nm. (b) Images of cuvettes containing 5 mg of COF-18Å trapped in the folded filter paper at the bottom of the cuvette in the above listed solvents after the 1 h hydrolysis. The observed color is attributed to oxidization of THB after it is released from the framework.

quite rapidly resulting in the loss of the originally exhibited high degree of crystallinity and high surface areas. However, when alkyl substituents are present in the COF pores, hydrolysis is greatly retarded and the material maintains the persistent porosity for which it is most noted. Similar methods are being used to elucidate the stability of other COFs, including boroxine-linked networks, and linear polymers as well as to provide insight into the repair ability of COFs and their environmental stability toward defining potential applications. Additional studies are underway to evaluate the steric and electronic contribution of these alkyl substituents toward COF stabilization.

EXPERIMENTAL SECTION

Materials. Benzene-1,3,5-triboronic acid (TBA),[1b] 1,2,4,5-tetrahydroxybenzene (THB),[18] 3,6-diethyl-1,2,4,5-tetrahydroxybenzene (DETHB),[1c] COF-18Å,[1b] COF-16Å, COF-14Å, and COF11Å[1c] were synthesized as described previously. COF-5 was prepared in an open round-bottom flask with condenser (rather than the sealed tube) in tetrahydrofuran/methanol (rather than mesitylene/1,4-dioxane) analogous to the COF-18Å family. All absorbance-based hydrolysis tests used Fisherbrand P8, coarse, fast filter paper (Cat. No. 09-795B). All reagents were purchased from Acros and used without further purification. All solvents used were obtained from solvent purification systems from Innovative Technologies.

Instrumentation. Solution ^{1}H NMR spectra were collected on a Varian Mercury/VX 400 MHz spectrometer. Gas adsorption data were collected with a Quantachrome Autosorb-1 automated adsorption analyzer. After activating the COFs as described below, they were independently loaded into a 6 mm sample cell (small bulb) and degassed at 400 °C under high vacuum (<0.001 mmHg) for 6−18 h. Data was obtained using a liquid nitrogen bath (77 K), with nitrogen gas as the adsorbate. Powder X-ray diffraction data were collected on a Rigaku DMax 2200 using Cu Kα radiation. Data were collected from 2 to 70° 2θ with steps of 0.05° with a count time of 12 s per step. After grinding the obtained solids using a mortar and pestle, the fine powders were dried on a vacuum line (0.3−0.5 mmHg) at ambient temperature for approximately 1−2 h. The sample was mounted in a deep well glass slide and analyzed. SEM images were obtained using a FEI Quanta Environmental Scanning Electron Microscope in high vacuum mode using 20 kV accelerating voltage. Clean, ground COF powder samples were mounted on double-sided carbon tape on aluminum sample holders. Absorbance studies were performed using a Beckman Coulter DU 640 spectrophotometer using quartz cuvettes from Starna (Cat. No. 3-Q10-GL14-S).

General Procedure for the Formation of COFs. Benzene-1,3,5-triboronic acid (TBA) (1 equiv) and the corresponding bis-diol (2 equiv) were dissolved in a mixture of tetrahydrofuran (THF) (19.8 mL/mmol acid) and methanol (0.2 mL/mmol acid). The solution was refluxed under constant nitrogen flow and monitored for 3 days during which solid COF formed on the glass walls. Additional THF was added as needed to maintain the original solvent level. The reaction mixture was cooled to room temperature and the fine suspension formed was collected by filtration. The solid was rinsed with THF (50 mL) and dried under vacuum (0.5 mmHg) for 24 h. COFs were activated for analysis by suspending 25−50 mg of each COF in 3 mL of dry THF. After 24 h, the solvent was decanted and an additional 3 mL of THF was added to the vial. After another 24 h, the solvent was again decanted and the sample was dried on a vacuum line (0.3−0.5 mmHg) at ambient temperature for 24 h. The resulting dried powder was ground with mortar and pestle for immediate use.

Hydrolysis Test by ^{1}H NMR. Into an NMR tube, 1 mg of clean, dry, activated, and ground COF was placed. D_2O (0.7 mL) and 1 μL benzene (internal standard) were added and NMR scans were run periodically for 60 min, and then extending up to 1 week to monitor the growth of the hydrolyzed monomer peaks.

Hydrolysis Test by Absorbance. Onto a 1 cm × 2 cm rectangle of filter paper, 5 mg of clean, dry, activated, and ground COF was carefully weighed. The filter paper was folded in half and the edges were folded closed with tweezers to enclose the COF. The resulting square envelope was placed flat onto the bottom of a 1 cm quartz cuvette with the folds facing the bottom of the cuvette. Immediately prior to the first scan, 3 mL of solvent was carefully added dropwise to the cuvette. Intermittent absorbance scans were taken without moving the cuvette. The UV−vis light beam was transmitted through the sample in the bottom 1 cm of the cuvette, above the level of the filter paper trap. All data were collected at 25 °C.

ASSOCIATED CONTENT

Supporting Information. Absorbance spectra of monomers, COF-18Å, and COF-5 in various solvents, the autooxidation product of THB, COF-18Å in dioxane over extended time; and half-life calculations. This material is available free of charge via the Internet at http://pubs.acs.org.

AUTHOR INFORMATION

Corresponding Author
lavigne@chem.sc.edu

ACKNOWLEDGMENT

Financial support for this work was provided by the National Science Foundation (CHE-0718877). The authors would like to acknowledge the University of South Carolina Electron

Microscopy Center for instrument use, and scientific and technical assistance.

REFERENCES

(1) (a) Cote, A. P.; Benin, A. I.; Ockwig, N. W.; O'Keeffe, M.; Matzger, A. J.; Yaghi, O. M. *Science* **2005**, *310*, 1166–1170. (b) Tilford, R. W.; Gemmill, W. R.; zur Loye, H.-C.; Lavigne, J. J. *Chem. Mater.* **2006**, *18*, 5296–5301. (c) Tilford, R. W.; Magavero, S. J., III; Pellechia, P. J.; Lavigne, J. J. *Adv. Mater.* **2008**, *20*, 2741–2746. (d) Cote, A. P.; El-Kaderi, H. M.; Furukawa, H.; Hunt, J. R.; Yaghi, O. M. *J. Am. Chem. Soc.* **2007**, *129*, 12914–12915. (e) Wan, S.; Guo, J.; Kim, J.; Ihee, H.; Jiang, D. *Angew. Chem., Int. Ed.* **2008**, *47*, 1–5. (f) Hunt, J. R.; Doonan, C. J.; LeVangie, J. D.; Cote, A. P.; Yaghi, O. M. *J. Am. Chem. Soc.* **2008**, *130*, 11872–11873.

(2) (a) Zhao, D.; Timmons, D. J.; Yuan, D.; Zhou, H.-C. *Acc. Chem. Res.* **2011**, *44*, 123–133. (b) Meek, S. T.; Greathouse, J. A.; Allendorf, M. D. *Adv. Mater.* **2011**, *23*, 249–267. (c) Christoph Janiak, C.; Vieth, J. K. *New J. Chem.* **2010**, *34*, 2366–2388. (d) Long, J. R.; Yaghi, O. M., Guest Eds. *Chem. Soc. Rev.* (Special Issue) **2009**, *38*, 1201−1508. (e) Mueller, U.; Schubert, M.; Teich, F.; Puetter, H.; Schierle-Arndt, K.; Pastre, J. J. *Mater. Chem.* **2006**, *16*, 626–636. (f) Rowsell, J. L. C.; Yaghi, O. M. *Angew. Chem., Int. Ed.* **2005**, *44*, 4670–4679. (g) Rowsell, J. L. C.; Yaghi, O. M. *Microporous Mesoporous Mater.* **2004**, *73*, 3–14. (h) Yaghi, O. M.; O'Keeffe, M.; Ockwig, N. W.; Chae, H. K.; Eddaoudi, M.; Kim, J. *Nature (London, U.K.)* **2003**, *423*, 705–714. (i) *Handbook of Porous Solids*; Schüth, F., Sing, K. S. W., Weitkamp, J., Eds.; Wiley- VCH: Weinheim, Germany, 2002. (j) Férey, G. *Chem. Mater.* **2001**, *13*, 3084–3098.

(3) Furukawa, H.; Yaghi., O. M. *J. Am. Chem. Soc.* **2009**, *131*, 8875–8883.

(4) (a) Niu, W.; Smith, M. D.; Lavigne, J. J. *J. Am. Chem. Soc.* **2006**, *128*, 16466–16467. (b) Rambo, B. M.; Lavigne, J. J. *Chem. Mater.* **2007**, *19*, 3732–3739. (c) Nyilas, E.; Soloway, A. H. *J. Am. Chem. Soc.* **1959**, *81*, 2681–2683. (d) Hall, L. W.; Odom, J. D.; Ellis, P. D. *J. Am. Chem. Soc.* **1975**, *97*, 4527–4531. (e) Bachler, V.; Metzler-Nolte, N. *Eur. J. Inorg. Chem.* **1998**, 733–744. (f) Good, C. D.; Ritter, D. M. *J. Am. Chem. Soc.* **1962**, *84*, 1162–1166. (g) Matteson, D. S. *J. Am. Chem. Soc.* **1960**, *82*, 4228–4233.

(5) Niu, W.; O'Sullivan, C.; Rambo, B. M.; Smith, M. D.; Lavigne, J. J. *Chem. Commun.* **2005**, 4342–4344.

(6) Cheng, Y.; Kondo, A.; Noguchi, H.; Kajiro, H.; Urita, K.; Ohba, T.; Kaneko, K.; Kanoh, H. *Langmuir* **2009**, *25*, 4510–4513.

(7) Yang, S. J.; Choi, J. Y.; Chae, H. K.; Cho, J. H.; Nahm, K. S.; Park, C. R. *Chem. Mater.* **2009**, *21*, 1893–1897.

(8) (a) Niu, W.; Rambo, B.; Smith, M. D.; Lavigne, J. J. *Chem. Commun.* **2005**, 5166–5168. (b) Niu, W.; Smith, M. D.; Lavigne, J. J. *Cryst. Growth Des.* **2006**, *6*, 1274–1277.

(9) Han, S. S.; Furukawa, H.; Yaghi, O. M.; Goddard, W. A., III. *J. Am. Chem. Soc.* **2008**, *130*, 11580–11581.

(10) Zwaneveld, N. A. A.; Pawlak, R.; Abel, M.; Catalin, D.; Gigmes, D.; Bertin, D.; Porte, L. *J. Am. Chem. Soc.* **2008**, *130*, 6678–6679.

(11) Campbell, N. L.; Clowes, R.; Ritchie, L. K.; Cooper, A. I. *Chem. Mater.* **2009**, *21*, 204–206.

(12) See Supporting Information.

(13) Brunauer, S.; Emmett, P. H.; Teller, E. *J. Am. Chem. Soc.* **1938**, *60*, 309–319.

(14) It is worth mentioning that the initial (i.e., prehydrolysis) surface area measurements for each COF have been measured numerous times by many different researchers and always provide values similar to those previously reported. The post-hydrolysis values were measured once each. However, the absorbance and NMR evaluations were carried out in replicate and consistently afforded the same results. Ultimately, it is the general trend that is of interest and importance here and not the absolute values reported, and these are consistent across evaluation methods.

(15) Note: for COF-5, the dried THF wash was used for the post-hydrolysis test.

(16) Evidence for the formation of this proposed auto-oxidation product was observed with the appearance of an absorbance peak centered near 490 nm.

(17) (a) Steenken, S.; Neta, P. *J. Phys. Chem.* **1979**, *83*, 1134–1137. (b) Joslyn, M. A.; Branch, G. E. K. *J. Am. Chem. Soc.* **1935**, *57*, 1779–1785.

(18) Weider, P. W.; Hegedus, L. S.; Asada, H.; D'Andreq, S. V. *J. Org. Chem.* **1985**, *50*, 4276–4281.